J. Fluid Mech. (1977), *vol.* 80, *part* 4, *pp.* 641–671
Printed in Great Britain

The hydraulics of rotating-channel flow

By A. E. GILL

Department of Applied Mathematics and Theoretical Physics, University of Cambridge

(Received 24 June 1976 and in revised form 25 November 1976)

Flow of a homogeneous inviscid fluid down a rotating channel of slowly varying cross-section is considered, with particular reference to conditions under which the flow is 'hydraulically controlled'. This problem is a member of a general class of problems of which gas flow through a nozzle and flow over a broad-crested weir are examples (Binnie 1949). A general discussion of such problems gives the means for determining the position of the control section (which is generally flow dependent) and shows that at this position there always exist long-wave disturbances with zero phase speed (i.e. disturbances are always 'critical' at the control section). The general theory is applied to the rotating-channel problem for the case of uniform potential vorticity. For this problem, three parameters are needed to specify the upstream flow, and the control theory gives a relationship between these parameters which depends on the geometry of the channel.

1. Introduction

The deep ocean is naturally divided into a set of basins by the ridges which run across it. Often dense water accumulates on one side of a ridge, which acts like a dam. The depth to which the dense water can rise is limited because flow will eventually take place across a low point in the ridge (the 'sill') into the adjoining basin. The density distributions in the neighbourhoods of such sills, and the rates of flow, where estimates are available, suggest that the level of dense water in the upstream basin and the rate of flow from one basin to another may be 'hydraulically controlled' by mechanisms similar to those which control flows from dams and reservoirs. For instance, figure 1 shows a simplified picture of a temperature section across a sill (normal to the axis of the ridge) in the Caribbean Sea. The upper boundary of the dense water, as shown by the 3·9° isotherm, has a configuration similar to that shown by the free surface when water flows out of a reservoir.

In flows in the deep ocean, effects of the rotation of the earth are important because the scale is large and buoyancy effects are small compared with those for a typical dam. This led Whitehead, Leetmaa & Knox (1974) to investigate the hydraulics of a rotating fluid by means of laboratory experiment and a simple theory, which proved quite effective. However, their theory was restricted to cases where the flow comes from a basin which is so deep that the absolute vorticity is effectively zero. The flow upstream of a sill in the deep ocean seems unlikely to have this property, so it was felt important to consider a wider class of flows with non-zero potential vorticity. Second, the solution with hydraulic control was obtained by using a maximization principle applied as an empirical rule which is known to work for non-rotating flows. Therefore it was felt that the maximization principle required justification, and so part of this

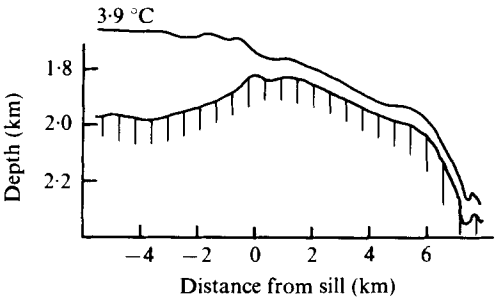

FIGURE 1. The configuration of the 3·9 °C potential-temperature surface in a section across the Jungfern Sill (adapted from Stalcup, Metcalf & Johnson 1975, figure 2). The section is roughly down the axis of the channel which crosses the ridge separating the Virgin Island Basin in the Caribbean from the Venezuelan Basin. The fluid below the 3·9 °C surface is colder (3·7–3·9 °C) and denser than the fluid above and flows from left to right in the diagram. The hatched area marks the bottom profile.

paper is addressed to this question in fairly general terms. (Stern (1974) made some comments about the maximization principle for the special case of zero absolute vorticity, but felt that this criterion would not be applicable to cases of finite potential vorticity.)

The discussion in this paper is restricted to a single layer of inviscid fluid of uniform density flowing under gravity in a rotating channel of slowly varying cross-section. This is, of course, a considerable simplification of the naturally occurring situation, but it thought to contain the most important ingredients for an understanding of what is observed in many cases. The first part of the paper is concerned with the general theory of 'hydraulics' type problems, and is introduced by a discussion of non-rotating channel flow, as this proves to be a convenient way to introduce the concepts involved and also some of the notation. Study of flow in a rotating channel begins in §4 and the basic equation relating a flow variable to the geometry of the channel is obtained in §5.

It is found that *three* parameters are required to describe the flow far upstream, where the channel is assumed to be very wide but of finite depth. Because of rotation, the flow is not distributed evenly over the cross-section, but is confined to boundary layers against the two walls (these are called the left bank and the right bank, the observer facing downstream towards the sill). The flux in each layer can be specified independently, giving two of the parameters. The third is the fluid depth away from the boundary layers, this corresponding to the prescribed potential vorticity. When the flow is hydraulically controlled, these three parameters will be related in a way which depends on the geometry of the channel.

The flow studied in this paper is assumed to vary slowly with downstream distance, i.e. changes with downstream distance are assumed to be significant only over distances large compared with the width. This assumption is not satisfied in the experiments of Whitehead *et al.* (1974) because there is a sudden change in depth at the entrance to the channel. Hydraulic control in a rotating system was also considered by Sambuco & Whitehead (1976), but there the assumption was that changes with y were rapid compared with those with x.

A result of the general hydraulics theory of §3 is that *long-wave* disturbances always

have zero phase speed at the control section, i.e. the Froude number is always unity there. In §6, the phase speed of long-wave disturbances is found for any section, the disturbed flow being assumed to have the original value of the potential vorticity. Hence a Froude number can be calculated as a function of distance down the channel for any solution.

The solutions for the rotating-channel problem are presented in various forms in §§8–12. In particular, §9 gives the formulae used for computing controlled flow solutions, and §10 gives some approximations to these solutions. A pictorial representation of some solutions may be found in §12.

2. Non-rotating hydraulics

The problem to be considered, i.e. steady flow down a rotating channel whose cross-section is slowly varying, is a generalization of the same problem for a non-rotating system. In fact, the non-rotating case can be regarded as the limit of the former problem as the rate of rotation tends to zero. To prepare the way for the more general problem it is useful first to discuss the concepts of the familiar non-rotating case in a manner which makes the generalization to the rotating case fairly straightforward. The discussion also serves to introduce some notation which will be useful later.

Consider the flow of a fluid of uniform density ρ down a channel of rectangular cross-section (figure 2). Let the y axis point downstream along the channel axis, let the z axis point vertically upwards and let the x axis be chosen such that the co-ordinates (x, y, z) form a right-handed system. Let $z = \eta$ be the elevation of the free surface and $z = -h$ be the level of the bottom of the channel. Then

$$D = h + \eta \tag{2.1}$$

is the depth of fluid in the channel. Let w be the width of the channel, so that the sides are at $x = \pm \frac{1}{2}w$, and let g be the acceleration due to gravity. The analysis may also be applied to a two-fluid system when the lower layer has depth D and the upper layer is very deep. Then $z = \eta$ is the height of the interface and g is the *reduced* gravity, i.e. gravity reduced by the fractional change in density across the interface. A discussion of the hydraulics of such a system may be found in Long (1972) and also in a film by Long (see National Committee for Fluid Mechanics Films 1972, pp. 136–142, MIT Press).

The channel dimensions h and w and the direction of the channel axis are assumed to vary so slowly that the flow in each section is effectively parallel to the y axis and has a velocity v which is uniform across the section. Let Q be the volume of fluid crossing any section per unit time. Then the flow is governed by two equations: the equation of continuity

$$Dwv = Q \tag{2.2}$$

and Bernoulli's equation

$$\tfrac{1}{2}v^2 + g\eta = g\eta_\infty, \tag{2.3}$$

where η_∞ is a constant, equal to the surface elevation where the flow velocity is zero. For flow from a large reservoir

$$Dw \to \infty \quad \text{as} \quad y \to -\infty \tag{2.4}$$

and so, by (2.2),

$$v \to 0 \quad \text{as} \quad y \to -\infty \tag{2.5}$$

and thus

$$\eta \to \eta_\infty \quad \text{as} \quad y \to -\infty, \tag{2.6}$$

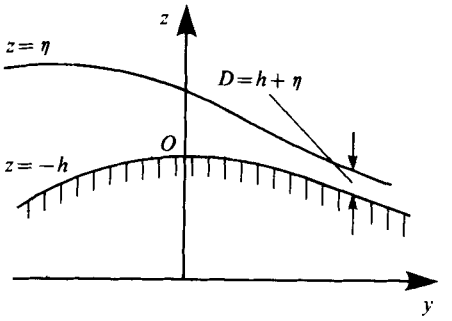

FIGURE 2. The co-ordinate system, illustrated by a section down the axis $x = 0$ of the channel. The z axis points vertically upwards and the y axis down the channel in the direction of flow. The surface is at $z = \eta(x, y)$ and the channel floor at $z = -h(x, y)$. $D = h + \eta$ is the depth of fluid.

i.e. η_∞ is the surface elevation far upstream, relative to the level $z = 0$. A convenient choice for this reference level ($z = 0$) is the highest point in the channel floor.

An alternative form of (2.3) is, by (2.1),

$$\tfrac{1}{2}v^2 + gD = g(h + \eta_\infty), \tag{2.7}$$

which can be combined with (2.2) to give an equation in a single dependent variable, D (or v). The equation for D is

$$gD + \tfrac{1}{2}Q^2/w^2D^2 = g(h + \eta_\infty), \tag{2.8}$$

a cubic equation which can be solved for D given w, h, η_∞ and Q. If the geometry is fixed, i.e. $w(y)$ and $h(y)$ are fixed, and the flow rate Q is specified, there is a one-parameter family of solutions corresponding to different possible upstream levels η_∞.

A convenient form of solution is one in terms of the non-dimensional quantities

$$D^* \equiv (gw^2/Q^2)^{\frac{1}{3}} D, \quad h^* \equiv (gw^2/Q^2)^{\frac{1}{3}} (h + \eta_\infty), \tag{2.9}$$

which, by (2.8), satisfy the cubic equation

$$h^* = D^* + \tfrac{1}{2}D^{*-2}, \tag{2.10}$$

whose graph is shown in figure 3. For a given value of the independent variable h^* there are two possible values of the dependent variable D^* when $h^* > \frac{3}{2}$, no possible values when $h^* < \frac{3}{2}$ and a single possible value $D^* = 1$ when $h^* = \frac{3}{2}$. The two branches of the curve are marked AB and BC in the figure and B marks the point $h^* = \frac{3}{2}$, $D^* = 1$, where the two branches meet.

Consider a geometry in which h^* is large at points far upstream, in conformity with (2.4), then reduces to a minimum value

$$h_m^* = \min h^* \tag{2.11}$$

at a certain point, which can be chosen as the origin $y = 0$ of the y axis, and finally increases again. By (2.9), the minimum can be due to a minimum in depth, a minimum in width or a combination of the two. When the width and depth both vary, the position of the special point $y = 0$ (sometimes called the control point) is uniquely defined by (2.11). Note that h_m^* depends on the upstream level η_∞ and so can be regarded as a non-dimensional parameter which measures the upstream level.

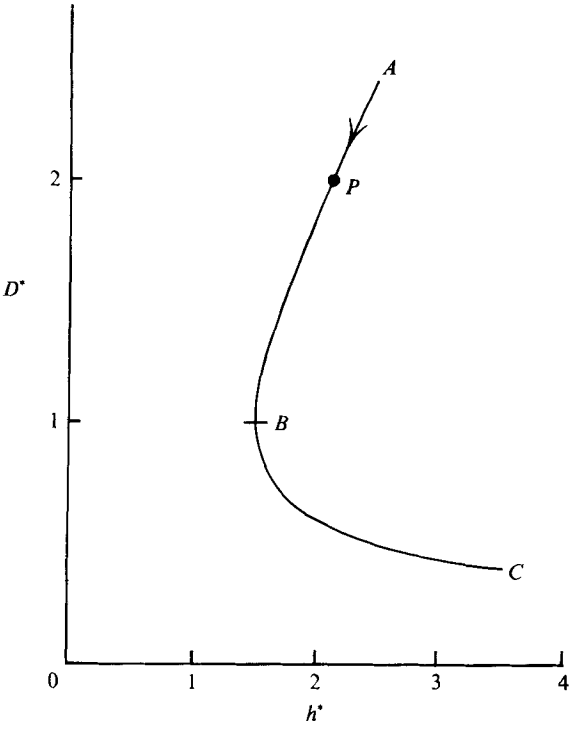

FIGURE 3. The relationship between the flow variable D^*, which is a measure of water depth, and the geometric parameter h^*, which depends on the width, flow rate, and depth relative to the upstream level. This is sometimes called the specific energy curve or specific head curve. The curve has two branches, which meet at the point B, where $D^* = 1$, $h^* = \frac{3}{2}$.

The way in which D_*, which measures the water depth, varies with y can be deduced from figure 3. The point $y = -\infty$ corresponds to the point A at infinity along the branch for which

$$D^* \sim h^* \quad \text{as} \quad h^* \to \infty. \tag{2.12}$$

As y increases, h^* decreases and so the solution follows the curve in the direction of the arrow until the point P, where $h^* = h_m^*$ is reached. A further increase in y corresponds to an increase in h^*, so the solution *retraces* the curve back towards A, and remains on the branch AB.

For large η_∞, h_m^* is large. As η_∞ is reduced, h_m^* reduces and so the point P eventually coincides with B, the turning point of the cubic, where

$$h_m^* = \tfrac{3}{2}. \tag{2.13}$$

This is a special case, because when y increases beyond zero the solution could follow either branch as h^* increases, i.e. towards A or towards C. For smaller values of η_∞, h_m^* is less than $\frac{3}{2}$, so the point B is reached at a negative value of y and no solution exists for values of y beyond this point.

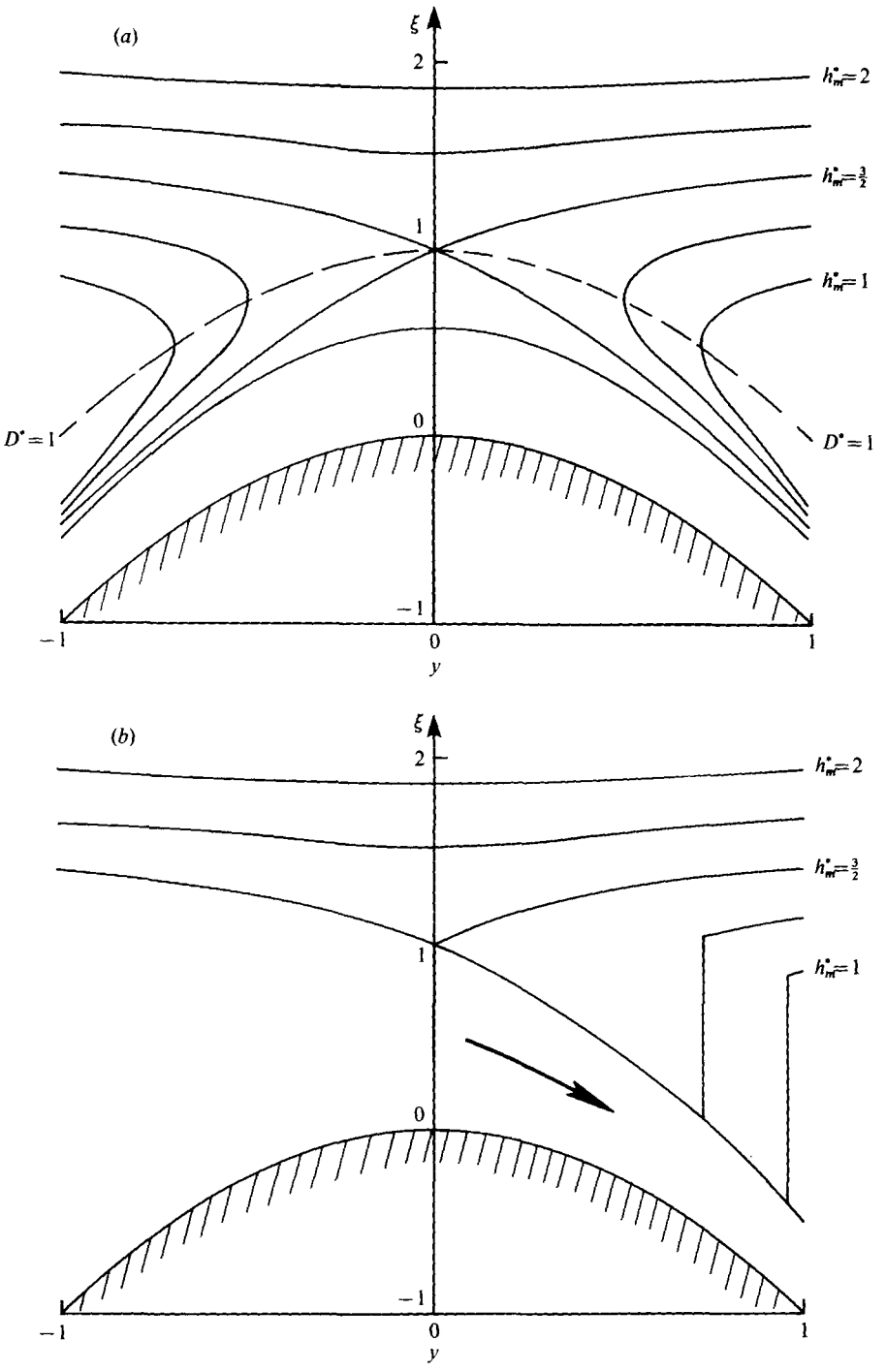

FIGURE 4. (*a*) The family of channel-flow solutions given by the theory for a channel of slowly varying cross-section. For channels of constant width, the hatched region represents the bottom and the solid lines configurations of the free surface. The broken line corresponds to a water depth $D^* = 1$. On this line the surface slope is infinite, contrary to the assumptions of the theory, except for the curves $h_m^* = \frac{3}{2}$. The solutions are symmetric about the centre-line. (*b*) The curves shown in (*a*) which contravene the assumptions of slowly varying flow must be modified by allowing for a rapid jump in level, i.e. a hydraulic jump. The position of the jump is determined by the requirement of no change in momentum flux and a loss (rather than a gain) of energy across the jump. The above shows the result obtained when flow is from left to right.

The situation may be seen more clearly in figure 4(*a*), which shows the family of possible solutions for a given geometry. The graph is drawn for the particular case

$$h^* = h_m^* + y^2, \tag{2.14}$$

but this represents no real loss of generality because y enters the solution only parametrically. Thus solutions for other profiles $h^*(y)$ are obtained merely by suitable stretching of the y axis. The ordinate ξ is defined by

$$\xi = h_m^* + D^* - h^* = h_m^* + (gw^2/Q^2)^{\frac{1}{3}}(\eta - \eta_\infty), \tag{2.15}$$

and so measures the surface elevation. In the particular case where the channel has constant width, figure 4(*a*) represents a section along the axis of the channel and the hatched region denotes the floor of the channel.

From (2.14) and (2.15), the surface elevation ξ and water depth D^* are related by

$$\xi = D^* - y^2. \tag{2.16}$$

Elimination of D^* and h^* from (2.16), (2.14) and (2.10) then gives the equation for the surfaces shown in figure 4(*a*), namely

$$\xi + \tfrac{1}{2}(\xi + y^2)^{-2} = h_m^*. \tag{2.17}$$

The point B, where the two branches of the cubic meet, is given by $D^* = 1$ and is shown by a broken line in figure 4(*a*). Curves with $h_m^* > \frac{3}{2}$ lie entirely above this line since they correspond to points on the branch AB of the cubic. Now the surface slope, from (2.16) and (2.17), is given by

$$\frac{d\xi}{dy} = \frac{1}{D^{*3} - 1}\frac{dh^*}{dy}, \tag{2.18}$$

and so is infinite on the broken line $D^* = 1$ *except* at the point $y = 0$, where dh^*/dy vanishes. At this point, the ratio on the right-hand side of (2.18) is replaced by the ratio of the derivatives, yielding [with the aid of (2.16)]

$$(d\xi/dy)^2 = \tfrac{1}{3}d^2h^*/dy^2, \tag{2.19}$$

so there are two possible slopes, as shown in the figure. There is *only one* curve (marked $h_m^* = \frac{3}{2}$) which satisfies the upstream condition and crosses the line $D^* = 1$ without an infinite surface slope. It is the only solution with a smooth transition from one branch of the cubic in figure 3 to the other. In other words, it is the only slowly varying flow for which the solution at a given h^* downstream ($y > 0$) of the minimum differs from the solution at the same h^* upstream ($y < 0$) of the point where h^* is a minimum.

Now consider the physical problem of flow from a large reservoir to which fluid is supplied at a uniform rate Q. What will be the surface level in the reservoir? The curve in figure 4(*a*) which is selected depends in practice on conditions applied at some downstream point, which effectively sets a surface level at some large value of y. Since

$$\xi \to h_m^* \quad \text{as} \quad y \to \infty \tag{2.20}$$

h_m^* assumes the value which ξ has far downstream. If this value is large figure 4(*a*) shows that the surface is almost flat, save for a slight depression centred on the constriction at $y = 0$. As the downstream level (and hence h_m^*) is lowered the depression

deepens and the curvature of the surface at $y = 0$ increases, tending to infinity as $h_m^* \downarrow \frac{3}{2}$. Up to this point, the surface level in the reservoir assumes the same value as is set downstream. But what happens when the downstream level is further reduced? If the downstream level is very low, e.g. on the lower curve $h_m^* = \frac{3}{2}$, then the appropriate curve is $h_m^* = \frac{3}{2}$ with the high level on the left, a smooth transition through $y = 0$ and low levels on the right. This suggests that the left-hand upper curve $h_m^* = \frac{3}{2}$ represents the lowest possible level in the reservoir, being obtained with a downstream level corresponding to either of the right-hand curves $h_m^* = \frac{3}{2}$. One might guess that the curve on the left is also the same for all downstream levels in between, but solution of the problem for such cases requires further consideration.

For such downstream levels, the curve in figure 4 (*a*) can be traced upstream (from $y = +\infty$) a certain distance, but the surface gradient eventually becomes very large and the assumption of slow variation with y breaks down. Hence there must be some relatively rapid transition, which in practice is called a *hydraulic jump* and takes on a form which is well known from observation. Here there is a loss of energy, proportional to the difference between the upstream value $\frac{3}{2}$ of h_m^* and the downstream value of h_m^* determined by the downstream level. The jump is not positioned at the point of infinite gradient, because the *momentum flux* (including the pressure term) at the jump must be continuous. Since this flux is given by

$$\tfrac{1}{2}gwD^2 + v^2Dw = (gQ^4/w)^{\frac{1}{3}}(\tfrac{1}{2}D^{*2} + D^{*-1}) \tag{2.21}$$

the value of

$$M = \tfrac{1}{2}D^{*2} + D^{*-1} \tag{2.22}$$

must be the same on either side of the jump. M has a minimum value of $\frac{3}{2}$ on the broken line $D^* = 1$ in figure 4 (*a*) and increases on either side. Figure 4 (*b*) shows the solutions which are consistent with the upstream reservoir condition, the downstream level condition and, where necessary, a single jump with M continuous and an energy loss. (It would be possible to have a jump upstream of the constriction with M continuous, but then energy would need to be supplied at the jump so this solution is rejected.)

Whenever the downstream level is below the upper $h_m^* = \frac{3}{2}$ curve the upstream level is invariably given by $h_m^* = \frac{3}{2}$. In such cases, the upstream level is said to be *controlled* by the constriction at $y = 0$ and the section $y = 0$ is called the control section. In engineering practice, the control section is a spillway or weir, and equipment is installed so that the geometry of the control section may be altered when it is desired to change the upstream level. In natural flows, e.g. when a river descends through a series of rapids, there will be a control section where h_* has the smallest value, then another where h_* has the next smallest value downstream and so on, thus determining the position of each rapid.

Another aspect of hydraulics theory concerns the behaviour of long-wave disturbances. These disturbances have wavelengths long enough for the flow at each section to be considered uniform and parallel to the axis, yet short enough so that changes in the dimensions of the channel over a wavelength can be ignored. At each section, there are two possible values of the phase speed c of the disturbances, given by

$$c = v \pm (gD)^{\frac{1}{2}}. \tag{2.23}$$

The ratio of the flow velocity v to the disturbance speed $|c-v|$ relative to the flow is called the *Froude number* F, and is given by

$$F = v/|c-v| = v/(gD)^{\frac{1}{2}} = D^{*-\frac{3}{2}}. \tag{2.24}$$

Thus for $D^* > 1$ (i.e. on the branch AB of the curve in figure 3), long-wave disturbances can travel both upstream and downstream, and the flow is said to be *subcritical* (i.e. $F < 1$). For $D^* < 1$ (i.e. on the branch BC of the curve in figure 3), long-wave disturbances can travel *only* in the downstream direction, and the flow is said to be *supercritical* (i.e. $F > 1$). When $F = 1$ the flow is said to be critical, and points where this occurs are called critical points. Since this occurs when $D^* = 1$, the control point is also a critical point, i.e. the change of branch of the curve in figure 3 occurs exactly at the point where $F = 1$, i.e. where there are long-wave disturbances which propagate neither upstream nor downstream ($c = 0$). In the next section, it will be shown that this is a general property of a wide class of flows.

The upper curves in figure 4 (*b*), which are symmetrical about $y = 0$, correspond to flow which is everywhere subcritical, so disturbances can carry information both upstream and downstream. For the remaining curves, the flow is subcritical upstream of the constriction, supercritical between the constriction and the hydraulic jump, and subcritical downstream of the jump. Thus, if any change is made at the constriction by altering the geometry, long waves can carry the information upstream. On the other hand, disturbances created at the hydraulic jump cannot propagate upstream because the flow is supercritical there.

3. General theory of 'hydraulics' type problems

There is a whole class of problems which have essentially the same character as the hydraulics problem considered in the last section. A list of such problems has been compiled by Binnie (1949) together with a discussion of their treatment and their history. The first problem in this class to be studied was that of gas flow through a nozzle (Hugoniot 1886; Reynolds 1886). The purpose of this section is to express these problems in a common form, and to show that stationary long-wave disturbances inevitably occur at the control point, i.e. that the flow is 'critical' there. In addition the arguments will be made more general than usual by considering a wider class of geometrical configurations.

A common feature of the problems to be considered is that a geometry is specified which involves a channel or tube with some sort of constriction. The arguments are not always applied to a channel or tube with solid boundaries, but sometimes to a stream tube within a larger flow. The dimensions of the tube or channel are supposed to vary slowly with downstream distance, so that the flow is approximately parallel to the sides. The flows considered are steady. Usually the flow is assumed to depend only on one geometrical property such as the cross-sectional area, but this is an unnecessary restriction. Instead it will be assumed that the geometry is given by a set of parameters $h, w, \ldots$, which could represent, for instance, the height h of a channel floor, the channel width w, etc. These parameters vary slowly with downstream distance y. There appear to be three essential features.

(i) The flow can be specified in terms of a *single* dependent variable D whose

dependence on y is entirely *implicit* in terms of the geometric parameters $h, w, \ldots$; that is

$$\mathscr{J}(h, w, \ldots; D) = \text{constant}. \tag{3.1}$$

(ii) The function $\mathscr{J}$ is *multiple-valued* in that for some range of values of $h, w, \ldots$ there is more than one value of D. The surface $\mathscr{J}$ = constant is also assumed to be smooth.

(iii) The geometry involves some sort of 'constriction' in the sense that

$$\mathscr{G} \equiv \frac{\partial \mathscr{J}}{\partial h}\frac{dh}{dy} + \frac{\partial \mathscr{J}}{\partial w}\frac{dw}{dy} + \ldots = 0 \tag{3.2}$$

at some point.

Assumption (i) in practice results from the slow variation of the geometry with y. In the non-rotating case, the function $\mathscr{J}$ is given by the cubic (2.10). Assumption (ii) results from the nonlinear character of the equations of motion and assumption (iii) is an essential feature of the geometry. When only one parameter h is needed, this third assumption reduces to the requirement that dh/dy vanishes at some point.

Now consider what deductions can be made for problems which satisfy the above three criteria. The first deduction is concerned with the conditions which determine the position of the control section. The discussion of non-rotating flow in a channel shows that such a point occurs where there is a smooth transition from one branch of the curve $\mathscr{J}$ to the other. Where D depends on more than one geometrical parameter, $\mathscr{J}$ is a *surface* in $D, h, w, \ldots$ space so we are concerned with a transition from one *sheet* of the surface to another. The line along which the separate sheets of the surface meet is given by

$$\partial \mathscr{J}/\partial D = 0. \tag{3.3}$$

The argument which determines the position of the control section was first used by Hugoniot (1886) in connexion with gas flow through a nozzle. Differentiation of (3.1) with respect to y gives

$$\frac{\partial \mathscr{J}}{\partial D}\frac{dD}{dy} = -\mathscr{G}, \tag{3.4}$$

so dD/dy is infinite and the solution breaks down where (3.3) is satisfied, unless $\mathscr{G} = 0$ at this point. Thus the control section is situated where (3.1)–(3.3) are all satisfied. At such a point, further differentiation of (3.4) gives

$$\frac{\partial^2 \mathscr{J}}{\partial D^2}\left(\frac{dD}{dy}\right)^2 = -\frac{\partial \mathscr{G}}{\partial y}, \tag{3.5}$$

so it is essential also that $\partial^2 \mathscr{J}/\partial D^2$ and $\partial \mathscr{G}/\partial y$ have opposite signs at this point. This condition distinguishes, in effect, a 'constriction' from an 'expansion'. In the case of non-rotating channel flow, (3.4) becomes (2.18) and (3.5) becomes (2.19). Note that when there is only one parameter h, the *position* of the control is given by (3.2), which becomes $dh/dy = 0$, and (3.3) determines the *character* of the flow at this point. The same is true if $dh/dy, dw/dy, \ldots$ vanish at the same point. In general, however, dh/dy, $dw/dy \ldots$ vanish at different points, and the control section must presumably lie at some point in between. Equation (3.2) determines where this point is, and shows that its position depends on the flow.

The other deduction which can be made is concerned with long-wave disturbances to the flow. Such disturbances have zero phase speed, i.e. are stationary, when (3.1) is

satisfied not only for the mean flow D but for the slightly disturbed flow $D+\delta D$. Therefore

$$\mathscr{J}(h, w, \ldots; D+\delta D) = 0$$

holds in addition to (3.1) and so (3.3) follows. Therefore stationary long-wave disturbances always exist at the control section. This explains why the Froude number is unity at this point in the non-rotating hydraulics problem, and why the Mach number is unity at the nozzle for gas flow.

4. Equations for flow in a rotating channel

Consider flow under gravity in a channel which rotates about the vertical z axis with uniform angular velocity $\frac{1}{2}f$. Co-ordinate axes fixed in the rotating frame will be used, with the same notation as in §2 (see figure 2). An important effect introduced by rotation is that the free surface slopes across the channel, so flow variables now depend on the cross-stream co-ordinate x as well as the downstream co-ordinate y. To begin with, the depth h of the channel floor below the co-ordinate plane $z = 0$ will also be allowed to depend on x, although detailed solutions will be calculated only for the case where h is independent of x.

If u and v are the velocity components in the x and y directions respectively, continuity implies the existence of a stream function ψ such that

$$Du = -\partial\psi/\partial y, \quad Dv = \partial\psi/\partial x. \tag{4.1a,b}$$

The velocity can be regarded as independent of depth since the horizontal scale is assumed to be large compared with the depth. The quantity $D(x, y)$ is the fluid depth defined by (2.1), and also in figure 2. The dynamic equations may be written in the form

$$-(f+\zeta)v = -\partial B/\partial x, \tag{4.2}$$

$$(f+\zeta)u = -\partial B/\partial y,$$

where

$$\zeta = \partial v/\partial x - \partial u/\partial y \tag{4.3}$$

is the vorticity relative to the rotating frame and

$$B = g\eta + \tfrac{1}{2}(u^2+v^2) \tag{4.4}$$

is the Bernoulli function. Equations (4.1) and (4.2) together imply that

$$B = B(\psi), \tag{4.5}$$

i.e. B is constant along streamlines. Equation (4.2) further implies that the potential vorticity (absolute vorticity divided by fluid depth) is given by

$$(f+\zeta)/D = dB/d\psi, \tag{4.6}$$

and so must also be constant along streamlines.

Now it is assumed that variations with downstream distance are on a scale large compared with the width of the channel, so that $u \ll v$ and $\partial u/\partial y \ll \partial v/\partial x$. Thus (4.4) and (4.6) simplify to

$$g\eta + \tfrac{1}{2}v^2 = B(\psi) \tag{4.7}$$

and

$$f + \partial v/\partial x = D\,dB/d\psi \tag{4.8}$$

respectively. In addition the x derivative of (4.7) together with (4.8) and (4.1b) implies the geostrophic balance

$$fv = g\,\partial\eta/\partial x \tag{4.9}$$

between the Coriolis acceleration and the cross-stream pressure gradient.

Equations (4.7)–(4.9) are difficult to handle in general because of their nonlinear form, but in the special case where the *potential vorticity* is *uniform* a linear equation is obtained. The rest of the paper is restricted to this special case, for which (4.8) becomes

$$\frac{f+\partial v/\partial x}{D} = \frac{f}{D_\infty}, \tag{4.10}$$

where D_∞ is a constant. D_∞ may be interpreted as the fluid depth at points where the relative vorticity ζ is zero. Alternatively, f/D_∞ is the given value of the potential vorticity, which may be regarded as a value associated with upstream conditions. Now the Bernoulli equation (4.7) becomes

$$g\eta + \tfrac{1}{2}v^2 = (f/D_\infty)\,\psi + g\eta_\infty, \tag{4.11}$$

where η_∞ is the surface elevation on the streamline $\psi = 0$ at points where the current v is zero. The stream function ψ will be defined such that

$$\psi = \pm\tfrac{1}{2}Q \quad \text{on} \quad x = \pm\tfrac{1}{2}w, \tag{4.12}$$

i.e. the streamline $\psi = 0$ has half the flow on either side.

The four governing equations (4.9)–(4.12) can be divided into two subsets. The first subset, comprising (4.9) and (4.10), gives a second-order equation, namely

$$\left(\frac{\partial^2}{\partial x^2} - \frac{f^2}{gD_\infty}\right)(D - D_\infty) = \frac{\partial^2 h}{\partial x^2}, \tag{4.13}$$

which determines the cross-sectional profiles of water depth and velocity. The width scale

$$w_s = 2(gD_\infty)^{\frac{1}{2}}/f \tag{4.14}$$

which appears in this equation is the *Rossby radius* of deformation based on the *upstream* potential vorticity f/D_∞, i.e. on the depth D_∞. When (4.13) is solved, the Bernoulli equation (4.11) can be applied at the two boundaries to give an equation of the form (3.1) relating flow characteristics to geometry.

The non-dimensional system of variables to be used will be based on the width scale w_s defined by (4.14), a velocity scale v_s and a depth scale D_s. v_s and D_s are chosen to satisfy

$$D_s w_s v_s = Q, \quad \tfrac{1}{2}fv_s = gD_s/w_s, \tag{4.15}$$

the first relationship being based on continuity and the second on the geostrophic balance. Thus D_s and v_s are given by

$$D_s = (\tfrac{1}{2}fQ/g)^{\frac{1}{2}}, \quad v_s = (\tfrac{1}{2}fQ/D_\infty)^{\frac{1}{2}}. \tag{4.16}$$

Non-dimensional variables are defined by

$$\hat{x} = \frac{x}{w_s}, \quad \hat{w} = \frac{w}{w_s}, \quad \hat{v} = \frac{v}{v_s}, \quad \hat{\psi} = \frac{\psi}{Q}, \quad \hat{D} = \frac{D}{D_s}, \quad \hat{h} = \frac{h+\eta_\infty}{D_s} \tag{4.17}$$

and the non-dimensional parameter which enters the problem will be denoted by

$$\hat{D}_\infty = D_\infty/D_s = (gD_\infty^2/\tfrac{1}{2}fQ)^{\frac{1}{2}} \tag{4.18}$$

or by

$$Q_* = \tfrac{1}{2}fQ/gD_\infty^2 = \hat{D}_\infty^{-2}. \tag{4.19}$$

The parameter Q_* can be regarded as the ratio of the actual flow rate Q to a flow rate based on a depth scale D_∞, a width scale equal to the Rossby radius based on D_∞ and a velocity scale $(gD_\infty)^{\frac{1}{2}}$ based on D_∞.

With these definitions, (4.9)–(4.13) become

$$\hat{v} = \frac{1}{2}\frac{\partial \hat{D}}{\partial \hat{x}} - \frac{1}{2}\frac{\partial \hat{h}}{\partial \hat{x}}, \tag{4.20}$$

$$\frac{1}{2}\frac{\partial \hat{v}}{\partial \hat{x}} = \hat{D} - \hat{D}_\infty, \tag{4.21}$$

$$\hat{D} - \hat{h} = \hat{D}_\infty^{-1}(-\tfrac{1}{2}\hat{v}^2 + 2\hat{\psi}), \tag{4.22}$$

$$\hat{\psi} = \pm\tfrac{1}{2} \quad \text{at} \quad \hat{x} = \pm\tfrac{1}{2}\hat{w}, \tag{4.23}$$

$$\frac{\partial^2 \hat{D}}{\partial \hat{x}^2} - 4(\hat{D} - \hat{D}_\infty) = \frac{\partial^2 \hat{h}}{\partial \hat{x}^2}. \tag{4.24}$$

5. The equation relating the flow to the geometry

The equations derived above will now be solved to give the profiles of surface elevation and velocity at any given section y = constant. These profiles depend on a single flow variable $\bar{D}$, and so an equation of the form (3.1) can be found which relates $\bar{D}$ to the parameters which define the geometry of the section. This equation will then be put in a form [cf. (2.17)] which explicitly gives the dependence on the parameters which specify the upstream flow.

Non-dimensional quantities will be used, but circumflexes will be dropped for the variables (4.17) from this point onwards [but will be retained for the parameter (4.18)]. For simplicity, attention will be restricted to the case of a channel of rectangular cross-section, i.e. one for which $\partial h/\partial x = 0$. The geometry is therefore specified by h and w, both of which vary with y in some prescribed way.

In discussing flow variables, a suffix '+' will denote the value on the right bank (facing downstream, towards $y = \infty$), i.e. at $x = +\frac{1}{2}w$, and the suffix '−' will denote the value on the left bank $x = -\frac{1}{2}w$. An overbar will denote the *average* of the values at the two sides, and δ before a variable will denote *half the difference* between its values at the sides. Thus

$$\bar{D} = \tfrac{1}{2}(D_+ + D_-), \quad \delta D = \tfrac{1}{2}(D_+ - D_-) \tag{5.1}$$

and similarly for v. Using this notation, the solution of (4.24) can be written in the form

$$D - \hat{D}_\infty = (\bar{D} - \hat{D}_\infty)\frac{\cosh 2x}{\cosh w} + \delta D \frac{\sinh 2x}{\sinh w}. \tag{5.2}$$

It follows from (4.20) that v is given by

$$v = (\bar{D} - \hat{D}_\infty)\frac{\sinh 2x}{\cosh w} + \delta D \frac{\cosh 2x}{\sinh w}. \tag{5.3}$$

Calculating $\bar{v}$ and δv from this equation gives

$$t\bar{v} = \delta D, \quad \delta v = t(\bar{D} - \hat{D}_\infty) \tag{5.4), (5.5}$$

where

$$t = \tanh w. \tag{5.6}$$

Equations (5.4) and (5.5) can be regarded as integrated forms of (4.20) and (4.21) respectively.

So far, the two variables $\bar{D}$ and δD are needed to determine the profiles (5.2) and (5.3). However, two more equations can be obtained by applying the Bernoulli equation (4.22) at the two walls. The *difference* between these two equations, after (5.4) and (5.5) have been used to express the result in terms of $\bar{D}$ and δD, gives

$$\bar{D}\,\delta D = 1, \tag{5.7}$$

so the single variable $\bar{D}$ is sufficient to determine the profiles. The *sum* of the two Bernoulli equations, when (5.4), (5.5) and (5.7) have been used to express this in terms of $\bar{D}$, gives the quartic equation

$$2\hat{D}_\infty(\bar{D}-h)+(t\bar{D})^{-2}+t^2(\bar{D}-\hat{D}_\infty)^2 = 0. \tag{5.8}$$

This has the required form (3.1) and reduces to the cubic equation (2.10) for the non-rotating case in the limit as $f \to 0$, other dimensional variables being kept fixed.

Now consider the upstream conditions. In the non-rotating case, it was sufficient to require that the cross-sectional area $Dw \to \infty$ as $y \to \infty$ without specifying whether D, w or both tend to infinity. In the rotating case, such a general condition is no longer appropriate. In fact, the usual idea behind the assumption of constant potential vorticity is that the fluid comes from a source region of constant depth $\hat{D}_\infty$ where the relative vorticity is zero. Therefore, in the rotating case it will be assumed that the *width* w (but not the depth) tends to infinity far upstream, i.e. $t \to 1$ as $y \to -\infty$. In this limit, the flow has a boundary-layer character, the widths of the layers being the Rossby radius. Outside these layers, the flow is quiescent and the solution of (4.20) and (4.21) is simply

$$v = 0, \quad D = \hat{D}_\infty. \tag{5.9}$$

In the boundary layers, on the other hand, the solution of (4.24) is

$$D = \hat{D}_\infty + (D_\pm - \hat{D}_\infty)\exp(\pm 2x - w). \tag{5.10}$$

Three dimensional quantities are needed to specify this upstream flow, a suitable set being (*a*) the upstream potential vorticity, given by the depth D_∞, (*b*) the flux in the right-hand boundary layer and (*c*) the flux in the left-hand boundary layer. These determine *two* non-dimensional quantities, a convenient pair being $\hat{D}_\infty$ (which depends on D_∞ and the *total* flux Q) and $\hat{\psi}_i$, which is defined as the value of the non-dimensional stream function ψ in the *interior* portion of the channel, i.e. away from the two boundary layers. The *ratio* of the left-bank flux to the right-bank flux is then

$$\tfrac{1}{2}+\hat{\psi}_i : \tfrac{1}{2}-\hat{\psi}_i$$

by (4.23).

All properties of the upstream flow are determined by these two parameters (which are distinguished by the circumflex). In particular, the upstream value h_u of h is obtained from the Bernoulli equation (4.22) applied in the interior, which gives

$$\hat{D}_\infty - h_u = 2\hat{D}_\infty^{-1}\hat{\psi}_i. \tag{5.11}$$

The upstream level of the channel floor provides a convenient reference level for the floor level at other points. Defining $\Delta(y)$ as the height of the channel floor above this level, h is given by

$$h = h_u - \Delta. \tag{5.12}$$

Substituting for h in (5.8) and using (5.11) gives the required equation, namely

$$4\hat{\psi}_i + 2\hat{D}_\infty(\Delta + \bar{D} - \hat{D}_\infty) + (t\bar{D})^{-2} + t^2(\bar{D} - \hat{D}_\infty)^2 = 0. \tag{5.13}$$

This gives the flow variable $\bar{D}$ as a function of the two geometric variables Δ and t and of the two upstream parameters $\hat{D}_\infty$ and $\hat{\psi}_i$.

6. Long-wave disturbances

Before calculating solutions of (5.13), the properties of long-wave disturbances will be briefly considered so that distinctions can be made between 'subcritical' and 'supercritical' flows. Perturbation quantities will be denoted by a prime. The y scale of the disturbances is assumed to be large compared with the cross-stream scale, yet small compared with the scale on which the geometry is changing. The potential vorticity of the disturbed flow is assumed to be the same as for the undisturbed flow, so the disturbance equation which takes the place of (4.10) or (4.21) is

$$\tfrac{1}{2}\partial v'/\partial x = D'. \tag{6.1}$$

In addition, the geostrophic relation [cf. (4.20)] gives

$$v' = \tfrac{1}{2}\partial D'/\partial x. \tag{6.2}$$

Combining these gives a hyperbolic equation like (4.24) and the method of §5 gives in place of (5.4) and (5.5) the results

$$t\bar{v}' = \delta D', \quad \delta v' = t\bar{D}', \tag{6.3), (6.4}$$

where t is defined by (5.6) as before.

The Bernoulli equation does not apply to the disturbance. Instead, the downstream component of the momentum equation is applied at the two side walls. Since the cross-stream component of velocity vanishes on the walls, this gives

$$\frac{\partial v'}{\partial t} + v\frac{\partial v'}{\partial y} = -\hat{D}_\infty \frac{\partial D'}{\partial y}. \tag{6.5}$$

For travelling-wave solutions $\partial/\partial t = -c\,\partial/\partial y$, where c is the wave speed, so (6.5) gives

$$\hat{D}_\infty D'_\pm + (v_\pm - c)\,v'_\pm = 0. \tag{6.6}$$

The difference between these two equations gives, in place of (5.7),

$$\bar{D}\,\delta D' + F^{-1}\bar{D}'\,\delta D = 0, \tag{6.7}$$

where the Froude number F is defined by

$$F = \bar{v}/(\bar{v} - c). \tag{6.8}$$

Finally, the sum of the two equations (6.6) gives the required expression for F, namely

$$F^{-2} = \bar{D}^3 t^2[(1 - t^2)\,\hat{D}_\infty + t^2\bar{D}). \tag{6.9}$$

The flow will be called subcritical when $F < 1$ and supercritical when $F > 1$.

7. Separation of the stream from the left bank

Before discussing solutions of (5.13), it is necessary to determine the range of values of the flow variable $\bar{D}$ for which the equation is applicable. In the non-rotating case the fluid depth was independent of x, so the only requirement was for the variable D^* to be non-negative. In the rotating case a condition on $\bar{D}$ must be found which ensures that the fluid depth is non-negative *across the whole section*. A *necessary* condition for this to be true is that the fluid depth

$$D_{\pm} = \bar{D} \pm \delta D = \bar{D} \pm 1/\bar{D} \tag{7.1}$$

at the two side walls is non-negative, i.e.

$$\bar{D} \geqslant 1. \tag{7.2}$$

This condition is also sufficient, for if (7.2) holds D is non-negative at the two walls. For D to be negative at an interior point, therefore, there would have to be a minimum value at which D was negative. But at a minimum $\partial^2 D/\partial x^2$ is positive, and so, by (4.24), $D > \hat{D}_\infty > 0$, contrary to the requirement. This completes the proof.

Now consider what happens to the stream when it reaches a point where $\bar{D} = 1$. Here the depth D_- on the left bank is zero, by (7.1), so the stream separates from the left bank at this point. Beyond the point of separation, the stream occupies only part of the channel and so has an effective width $w_e < w$. In other words, the stream will be found only in the region

$$\tfrac{1}{2}w - w_e < x < \tfrac{1}{2}w$$

and the channel floor in the remainder of the channel will be dry. Beyond the point of separation, a new equation is required to replace (5.13). This equation is easily found by applying (5.13) only to the part of the channel occupied by the stream. Then $\bar{D} = 1$ and t is replaced by t_e, where

$$t_e = \tanh w_e. \tag{7.3}$$

This gives

$$4\hat{\psi}_i + 2\hat{D}_\infty(\Delta + 1 - \hat{D}_\infty) + t_e^{-2} + t_e^2(1 - \hat{D}_\infty)^2 = 0. \tag{7.4}$$

It can also be shown that the Froude number is given by

$$F^{-2} = t_e^2[(1 - t_e^2)\hat{D}_\infty + t_e^2], \tag{7.5}$$

i.e. the formula obtained by putting $\bar{D} = 1$ and $t = t_e$ in (6.9).

Thus the equation relating flow properties to geometry is (5.13) when (7.2) is satisfied, but is replaced by (7.4) when (7.2) is not satisfied. The need for a different equation is purely a matter of description. Equation (5.13) is meaningful when the water surface intersects the side wall of the channel but must be replaced by (7.4) when the surface intersects the bottom. If the cross-section of the channel were not rectangular but, say, parabolic, the distinction between the 'side' and 'bottom' of the channel would not exist and so two different equations would not be necessary.

The separation of the stream from the bank occurs on the left side when the Coriolis parameter f is positive. The results for $f < 0$ can be obtained from those above merely by reversing the direction of the x axis (giving a left-handed co-ordinate system) but keeping D and v the same. Thus separation is from the right bank (facing downstream) when f is negative.

Note that 'downstream' refers to the direction of the total flux. It is possible that the flow in some parts of the channel may be in the opposite direction to the integrated flow. A useful indicator of how much v varies across the channel is the parameter

$$r = \delta v/\bar{v} = t^2\bar{D}(\bar{D} - \hat{D}_\infty). \tag{7.6}$$

A necessary condition for v to be non-negative everywhere is that the values $v_\pm = \bar{v} \pm \delta v$ at the two walls be non-negative, i.e. that

$$|r| \leqslant 1. \tag{7.7}$$

It can also be shown that this condition is *sufficient*. [The method is the same as that used for proving the sufficiency of (7.2).] When $r = 1$, $v_- = 0$ so there is a stagnation point on the left bank, and when $r > 1$ there is reverse flow adjacent to the left bank. On the other hand, $r = -1$ implies $v_+ = 0$, i.e. a stagnation point on the right bank, and $r < -1$ means that reverse flow occurs in the vicinity of the right bank.

8. Dependence of the flow variable on geometry

The behaviour of the flow in the *non-rotating* case was discussed in terms of the cubic (2.10) (see figure 3), which relates the flow variable D^* to the geometrical variable h^*. From the discussion in § 3, the essential property of this curve which allows hydraulic control is the existence of two branches. Now consider the corresponding curves for the rotating case. For a given geometry, $\Delta(y)$ and $t(y)$ will be specified so there will be a specified relation between Δ and t. Substituting in (5.13), a curve relating $\bar{D}$ to t (or Δ) can be obtained for given values $\hat{D}_\infty$ and $\hat{\psi}_i$ of the upstream parameters.

Figure 5 shows examples of such curves for the case of a flat-bottomed channel ($\Delta = 0$) of variable width when $\hat{\psi}_i = \frac{1}{2}$, i.e. when the upstream flux is entirely within the left-hand boundary layer. The curves were obtained by solving (5.13) for $\hat{D}_\infty$ and plotting contours of $\hat{D}_\infty$ in the $\bar{D}, t$ plane. All the curves have two branches. The flow obtained for different upstream levels can be discussed in the same way as for the non-rotating case (§ 2). Suppose, for instance, that the minimum width of the channel is given by $t = 0{\cdot}7$ ($w \approx 0{\cdot}9$). When the upstream level is high (look at the curves for $\hat{D}_\infty = 4$ and 3), $\bar{D}$ decreases very slightly from its upstream value (i.e. the value at $t = 1$) to its value at the constriction ($t = 0{\cdot}7$). Downstream of the constriction, t increases again and the only continuous solution is the one obtained by retracing the same curve back towards $t = 1$.

For smaller values of $\hat{D}_\infty$, the decrease in $\bar{D}$ between the upstream value and the value at the constriction increases until eventually a curve ($\hat{D}_\infty \approx 2{\cdot}1$) is reached which has a branch point at $t = 0{\cdot}7$. For this 'critical' value of $\hat{D}_\infty$, a change of branch is possible at the constriction. If this occurs, $\bar{D}$ continues to decrease downstream of the constriction even though t is increasing. However figure 5 shows that $\bar{D}$ decreases to unity before t has increased very much, so separation from the left bank will take place when the width reaches the corresponding value. Downstream of this point, the effective width of the stream remains constant.

Figure 6 shows another case where $\hat{\psi}_i = \frac{1}{2}$, but for which the height Δ of the channel floor varies. Imagine a channel which for $y < y_b$ has $\Delta = 0$ and a width gradually contracting to the value $w = 0{\cdot}75$ ($t = 0{\cdot}63$, $t^2 = 0{\cdot}4$) at $y = y_b$. For this part of the channel, figure 5 is appropriate. Figure 6 refers to the remainder of the channel

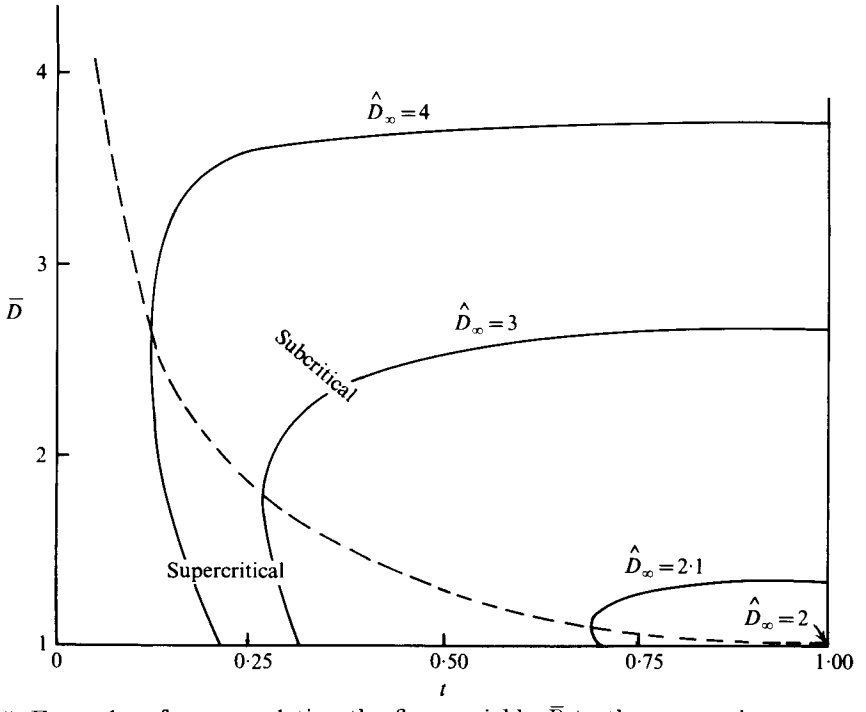

FIGURE 5. Examples of curves relating the flow variable $\bar{D}$ to the geometric parameter t (cf. figure 3), which is the hyperbolic tangent of the width. The channel floor in this case is flat, and $\hat{\psi}_i = \frac{1}{2}$, i.e. the upstream flow is all in a boundary layer on the left-hand wall, facing downstream. Solutions are meaningful only for $\bar{D} > 1$, since the flow separates from the left-hand wall at the point where $\bar{D} = 1$. Downstream of this point $\bar{D}$ remains equal to 1 and the width of the region occupied by fluid remains constant. Curves for other values of $\hat{\psi}_i$ for the flat-bottomed case also have a double-branched structure. The broken line is the locus of turning points where the two branches meet.

($y > y_b$), where the width is fixed ($w = 0{\cdot}75$) but Δ varies. The upper part of the figure shows how $\bar{D}$ varies with Δ in the permissible range $\bar{D} \geqslant 1$. (This was drawn simply by solving (5.13) for Δ given $\bar{D}$, $\hat{D}_\infty$ and t.) At $y = y_b$, $\Delta = 0$ and $\bar{D} > 1$, so the curve $\hat{D}_\infty =$ constant is entered on the upper left-hand border of figure 6. As y increases Δ increases, so the $\hat{D}_\infty$ contour is followed to the right. Since separation occurs if the point $\bar{D} = 1$ is reached, a curve showing dependence of the effective width w_e on Δ is required beyond this point. The lower panel of figure 6 shows such curves, $t_e = \tanh w_e$ being shown as a function of Δ (the curves were obtained by solving (7.4) for Δ given t_e and $\hat{D}_\infty$). If *both* parts of the figure are taken together, then each curve of constant $\hat{D}_\infty$ has two branches and hydraulic control is possible.

Consider examples where Δ increases from zero (at $y = y_b$) to a maximum value and then decreases to zero again. The line of maximum elevation of the channel floor will be called the sill, and the corresponding value of Δ the sill height. For low sills ($\max \Delta < 1{\cdot}5$), the separation point is in the subcritical region (above the broken line in figure 6) so separation (and subsequent reattachment) can occur even when there is no hydraulic control. Suppose, for instance, that the sill height is given by $\Delta = 3$, and consider a decreasing sequence of values of the upstream level $\hat{D}_\infty$. When $\hat{D}_\infty > 5{\cdot}1$

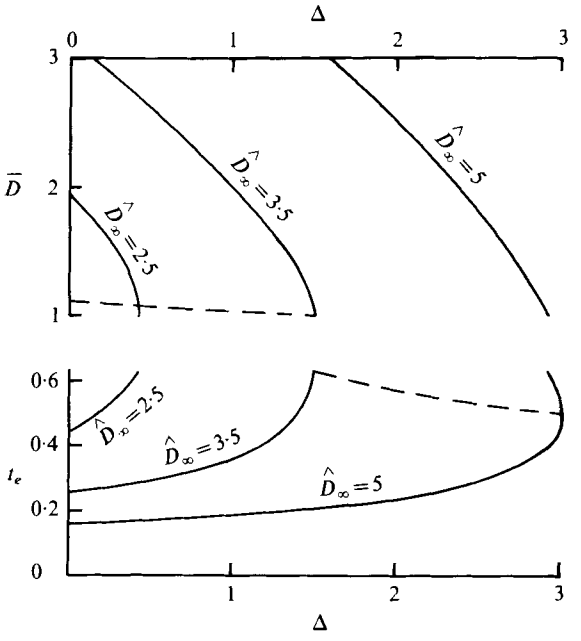

FIGURE 6. Dependence of flow properties on geometry for a channel of uniform width $w = 0{\cdot}75$ ($t = 0{\cdot}63$). The geometrical parameter which varies is Δ, the height of the channel floor. As in figure 5, $\hat{\psi}_i = \frac{1}{2}$, i.e. the upstream flow is all in the left-hand boundary layer. When the flow is not separated, the flow variable is $\bar{D}$. The upper part of the figure shows curves relating $\bar{D}$ and Δ for different values of the upstream level $\hat{D}_\infty$. The line $\bar{D} = 1$ marks where separation occurs. When the flow is separated, the flow variable is t_e, the hyperbolic tangent of the effective width. The lower part of the figure shows the relation between t_e and Δ. The broken line is the locus of points where a change of branch occurs. Above this line the flow is subcritical, below it is supercritical.

(the value for which $\Delta = 3$ when $\bar{D} = 1$), there is no separation and no change of branch. When $5{\cdot}0 < \hat{D}_\infty < 5{\cdot}1$, separation will occur for a small range of heights Δ near that of the sill, but there will be no transition. The critical value of $\hat{D}_\infty$ is 5. When $\hat{D}_\infty = 5$, separation occurs at the point where $\Delta = 2{\cdot}9$, but the flow is still subcritical until the sill ($\Delta = 3$) is reached. Here the effective width is given by $t_e = 0{\cdot}5$ and the flow becomes supercritical. Figure 6 then shows that, as Δ decreases again, t_e continues to decrease, eventually reaching a value of $0{\cdot}16$ when $\Delta = 0$.

The way in which figure 6 changes as t increases is rather interesting. The lower part of the figure is unchanged, but the range of relevant values of t_e increases. In other words, the lower panel extends further upwards. The value of Δ for which separation occurs at the sill decreases, the limiting value being zero when $t = 1$. As t changes, the curves in the upper panel change their shape. In particular, all contours of $\hat{D}_\infty$ become close to vertical at the point where $\bar{D} = 1$, indicating that proximity to transition does *not* occur at this point. Instead, the Froude number, which is only slightly less than unity at the separation point, decreases again [see (7.5)] to a minimum value of $2\hat{D}_\infty^{-1}(\hat{D}_\infty - 1)^{\frac{1}{2}}$ at the point where $2t_e^2 = \hat{D}_\infty(\hat{D}_\infty - 1)^{-1}$, then increases again, passing through unity at the point where $t_e^2 = (\hat{D}_\infty - 1)^{-1}$.

9. Controlled flow solutions

Curves like those shown in figures 5 and 6, which relate a flow variable to geometry, can be used to find solutions for *all* slowly varying flows, whether there is hydraulic control or not. From now on, however, attention will be restricted to the subset of these solutions for which the flow is controlled. The subscript c will be used to denote values at the control section, so Δ_c, for example, denotes the height of the channel floor at this point. Supposing that $\hat{\psi}_i$ is given, the problem is to find the value of the upstream parameter $\hat{D}_\infty$ for given geometry at the control section, i.e. for given values of Δ_c and t_c. The equation which determines the position of the control section is (3.3). This takes different forms depending on whether or not the flow at the control section is separated from the left bank, so the two cases will be considered individually.

Separated flow at the control section

The algebra is easier in this case, so it will be treated first. The relevant equation relating the flow variable t_e to the geometry is (7.4). When (3.3) is applied, the result which corresponds to a positive value of $\hat{D}_\infty$ is

$$\hat{D}_\infty = 1 + t_{ec}^{-2}, \tag{9.1}$$

where $t_{ec} = \tanh w_{ec}$ and w_{ec} is the effective width at the control section. The condition for this equation to be applicable is that w_{ec} is less than the actual width w_c at this section, i.e. $t_{ec} < t_c$ and so, by (9.1),

$$\hat{D}_\infty > 1 + t_c^{-2}. \tag{9.2}$$

Before going further, there is an interesting consequence of (9.1). Substituting for $\hat{D}_\infty$ in (7.6) and putting $\bar{D} = 1$, it follows that $r = -1$, i.e. there is a stagnation point on the right bank. In fact, substitution in (5.2) and (6.3) gives for the profiles at the control section

$$D = \frac{2[\cosh 2w_{ec} - \cosh(w_c - 2x)]}{\cosh 2w_{ec} - 1}, \tag{9.3}$$

$$v = \frac{\sinh(w_c - 2x)}{\sinh^2 w_{ec}}. \tag{9.4}$$

Thus the fluid depth D is 2 at the right bank, where the surface is horizontal ($\partial D/\partial x = 0$). The depth decreases monotonically with distance from the right bank, becoming zero when this distance equals w_{ec}. The velocity v is positive across the whole section, and increases monotonically from zero at the right bank to a maximum value of $(\sinh w_{ec})^{-1}$ at the point where the depth vanishes.

The way in which $\hat{D}_\infty$ depends on the geometry is found by eliminating the flow variable t_{ec} between (9.1) and (7.4). This gives

$$\Delta_c = \hat{D}_\infty - 2 + (1 - 2\hat{\psi}_i)\hat{D}_\infty^{-1}. \tag{9.5}$$

Solutions are shown in the upper part of figure 7. Note that the only dependence on t_c is through the requirement that (9.2) be satisfied. This implies that for a very wide channel (9.5) is applicable only in the range $\hat{D}_\infty > 2$ while for channels of finite width the cut-off value of $\hat{D}_\infty$ is even larger.

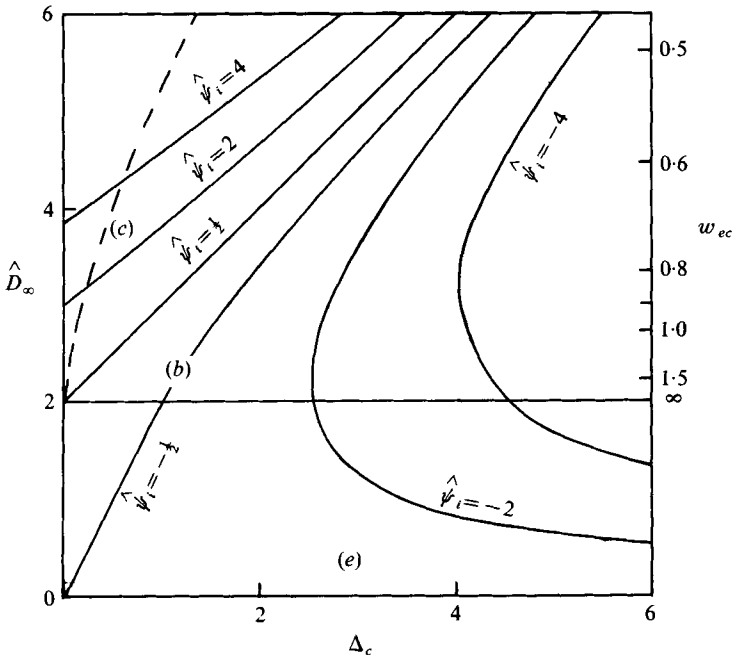

FIGURE 7. The solid curves show the relation between the upstream level $\hat{D}_\infty$ and the sill height Δ_c for controlled flow in the wide-channel limit ($t_c \to 1$). Each curve is for a fixed value of $\hat{\psi}_i$. Above the line $\hat{D}_\infty = 2$, flow at the control section is separated. To the upper left of the broken line, it is also separated at upstream infinity (but not so in the rest of the diagram). The effective width w_{ec} of the stream at the control section depends only on $\hat{D}_\infty$ [equation (9.1)]. Values of w_{ec} are indicated on the right. Below the line $\hat{D}_\infty = 2$, the flow at the control section is not separated. The point marked (*e*) corresponds approximately to the case depicted in figure 9(*e*) where $t = 0{\cdot}9$. When t_c is finite, the part of the diagram above the line $\hat{D}_\infty = 1 + t_c^{-2}$ is unchanged because the flow at the control section is still separated in those circumstances, and so the relationships are unaltered by a change of width. The points marked (*b*) and (*c*) correspond to the cases depicted in figures 9(*b*) and (*c*) respectively, where the flow is on the point of separating at the control section. The case shown in figure 9(*d*) features separated flow at the control section, but is off the scale in the above diagram ($\hat{D}_\infty = 18$, $\Delta_c = 16$).

Non-separated flow at the control section

In this case the flow variable is $\bar{D}$ and application of (3.3) to (5.13) gives

$$(1 - t_c^2)\,\hat{D}_\infty + t_c^2\,\bar{D}_c = \bar{D}_c^{-3}\,t_c^{-2}, \tag{9.6}$$

which, by (7.5), corresponds to unit Froude number. This equation applies when $\bar{D}_c \geqslant 1$ or, equivalently, whenever (9.2) is *not* satisfied. Note that (9.6) and (9.1) are identical when $\bar{D}_c = 1$. An important consequence of (9.6) is that flow at the control section is unidirectional, i.e. fluid particles in the control section cannot originate from downstream. This is a necessary condition for the solution to be physically meaningful, but turns out to be always satisfied. The proof is in the appendix.

The equations to be solved are (9.6) and (5.13), or (9.6) and the following equation obtained by adding $\bar{D}_c$ times (9.6) to (5.13) and dividing by $2\hat{D}_\infty$:

$$\Delta_c = (1 - \tfrac{1}{2}t_c^2)\,\hat{D}_\infty - \tfrac{3}{2}(1 - t_c^2)\,\bar{D}_c - (2\hat{\psi}_i + t_c^2\,\bar{D}_c^2)\,\hat{D}_\infty^{-1}. \tag{9.7}$$

Together (9.6) and (9.7) constitute an algebraic equation of order eight for $\hat{D}_\infty$ which

is difficult to solve explicitly. On the other hand, it is easy to construct solutions by regarding (9.6) and (9.7) as giving $\hat{D}_\infty$ and Δ_c implicitly as functions of $\bar{D}_c$ and t_c. For instance, tables can be constructed of $\hat{D}_\infty$ and Δ_c (and any derived quantities that may be wanted) as functions of D_c^{-1} and t_c, both these variables being confined to the range from zero to unity. Then $\hat{D}_\infty$ can be found as a function of Δ_c and t_c by interpolation.

10. Some limiting cases

The wide-channel limit ($t_c \to 1$)

By (9.2), the flow in this limit is separated if $\hat{D}_\infty > 2$, and then the solution is given by (9.5). If $\hat{D}_\infty \leqslant 2$, the flow is not separated and so solutions of (9.6) and (9.7) are required for small ϵ, where

$$\epsilon = 1 - t_c^2 \simeq 4\exp(-2w_c). \tag{10.1}$$

In this limit, (9.6) gives

$$\bar{D}_c = 1 + \tfrac{1}{4}\epsilon(2 - \hat{D}_\infty) + \tfrac{1}{32}\epsilon^2(36 - 20\hat{D}_\infty + 3\hat{D}_\infty^2) + \ldots, \tag{10.2}$$

showing that the flow is always close to separation at the control section even when $\hat{D}_\infty < 2$. When (10.2) is used in (9.7) the result is

$$\Delta_c = \frac{\hat{D}_\infty}{2} - \frac{1 + 2\hat{\psi}_i}{\hat{D}_\infty} + \epsilon\frac{\hat{D}_\infty^{-4}}{2} + \epsilon^2\frac{(5\hat{D}_\infty^2 - 14\hat{D}_\infty + 12)}{8\hat{D}_\infty} + \ldots. \tag{10.3}$$

The dependence of $\hat{D}_\infty$ on Δ_c in the limit is shown in figure 7. Above the line $\hat{D}_\infty = 2$, the flow is separated. The effective width w_{ec} at the control section is shown on the right and can be very much less than the actual width at the control section. Below the line $\hat{D}_\infty = 2$, the flow is not separated, so (10.3), with $\epsilon = 0$, replaces (9.5).

A description of the main features of the wide-channel controlled flow solutions can be obtained with the help of figure 7 and calculations of the flow properties far upstream. In the upper left part of figure 7 (the region bounded by the broken line), it turns out that the flow is separated even at upstream infinity. In the remainder of the figure, the upstream value $\bar{D}_u$ of $\bar{D}$ can be calculated by putting $\Delta = 0$ and $t = 1$ in (5.13) to give

$$\bar{D}_u^2 + \bar{D}_u^{-2} = \hat{D}_\infty^2 - 4\hat{\psi}_i. \tag{10.4}$$

The case $\hat{\psi}_i = \frac{1}{2}$ is a special one where the upstream flow is all contained in the left-hand boundary layer (so (10.4) gives the upstream value $\bar{D}_u + \bar{D}_u^{-1}$ of D_+ as $\hat{D}_\infty$). Then (9.5) gives the simple result

$$\hat{D}_\infty - \Delta_c = 2, \tag{10.5}$$

i.e. the upstream interior surface level is two units above the floor of the channel at the control section (it will be convenient to call this the sill). By (4.16), the dimensional form of this result is

$$D_\infty - \Delta_c = (2fQ/g)^{\frac{1}{3}}. \tag{10.6}$$

When $\hat{\psi}_i > \frac{1}{2}$, the upstream level is higher, as figure 7 shows. This case is interesting because the flow approaching the control section from far upstream is along the *left* bank (with flux $\frac{1}{2} + \hat{\psi}_i$), but at some point it separates and the unit flux which crosses the sill is in a stream against the *right* bank. The remaining flux is carried back towards upstream infinity in the right-hand boundary layer.

When $|\hat{\psi}_i| < \frac{1}{2}$, i.e. when the upstream flow is unidirectional, figure 7 shows that the flow at the control section is separated only when Δ_c is large enough. The upstream level is nearly two units above the sill, and approaches the value given by (10.5) as $\Delta_c \to \infty$. For small Δ_c the flow does not separate and (10.3) is approximated by

$$\hat{D}_\infty \approx (2 + 4\hat{\psi}_i)^{\frac{1}{2}} + \Delta_c. \tag{10.7}$$

When $\hat{\psi}_i < -\frac{1}{2}$, the upstream boundary-layer fluxes are in opposite directions, the right-hand layer containing the flux towards the sill. In this case the upstream interior level can be well *below* the sill level, but is also below the surface levels on the boundaries.

For cases where the channel is of large but finite width, the part of figure 7 in the region (9.2) is unaltered. Below this line, the curves are distorted slightly. The power series in ϵ given by (10.2) and (10.3) are useful even when the width approaches values as small as the Rossby radius ($w_c = 1$ corresponds to $\epsilon = 0{\cdot}42$).

The narrow-channel limit ($t_c \to 0$)

In this limit the flow is separated only for very large $\hat{D}_\infty$, as given by (9.2). Equation (9.5) shows that $\hat{D}_\infty$ is close to Δ_c unless $|\hat{\psi}_i|$ is large, so it is more useful to consider the differences $\hat{D}_\infty - \Delta_c$ rather than $\hat{D}_\infty$ itself. Thus (9.5) gives approximately

$$\hat{D}_\infty - \Delta_c \approx 2 + 2\hat{\psi}_i \hat{D}_\infty^{-1} \quad \text{for} \quad \hat{D}_\infty t_c^2 > 1, \tag{10.8}$$

the last term being important only when $|\hat{\psi}_i|$ is very large.

When (9.2) is not satisfied, the flow is governed by (9.6) and (9.7). If $\hat{D}_\infty \gg t_c$, the former gives

$$\bar{D}_c = \hat{D}_\infty^{-\frac{1}{3}} t_c^{-\frac{2}{3}} (1 + \tfrac{1}{3} t_c^2 - \tfrac{1}{3} \hat{D}_\infty^{-\frac{1}{3}} t_c^{\frac{4}{3}} \ldots) \tag{10.9}$$

and substitution in (9.7) then gives

$$\hat{D}_\infty - \Delta_c \approx \tfrac{1}{2} \hat{D}_\infty t_c^2 + \tfrac{3}{2} \hat{D}_\infty^{-\frac{1}{3}} t_c^{-\frac{2}{3}} + 2\hat{\psi}_i \hat{D}_\infty^{-1} \quad \text{for} \quad \hat{D}_\infty t_c^2 < 1. \tag{10.10}$$

As before, the last term is important only when $|\hat{\psi}_i|$ is large. If $|\hat{\psi}_i|$ is not large, the dimensional version of (10.8) and (10.10) is

$$D_\infty - \Delta_c \approx \begin{cases} (2fQ/g)^{\frac{1}{2}} & \text{for} \quad w_c^4 > gQ(\frac{1}{2}f)^{-3}, \\ \frac{3}{2}(Q^2/gw_c^2)^{\frac{1}{3}} + \frac{1}{8}(fw_c)^2/g & \text{for} \quad w_c^4 < gQ(4f)^{-3}. \end{cases} \tag{10.11}$$

The narrow-channel limit applies when the width of the control section is small compared with the Rossby radius, i.e. when the potential vorticity f/D_∞ is small compared with g/fw_c^2. Thus (10.11) is the result in the limit as the potential vorticity tends to zero. It is precisely the result obtained by Whitehead *et al.* [1974, equations (3.8) and (3.25)] for zero potential vorticity [they use the notation h_u for the left-hand side of (10.11)]. For small f, this reduces to the result for a non-rotating fluid.

If $\hat{\psi}_i \geqslant -\frac{1}{2}$ (10.11) gives the approximate solution for all Δ_c. If $\hat{\psi}_i < -\frac{1}{2}$, however, there are some additional small t_c solutions with $\hat{D}_\infty$ of order t_c. These solutions will not be discussed.

11. The case $\hat{\psi}_i = \frac{1}{2}$

The most useful application of the results obtained is probably to flow out of a basin, the exit channel being assumed to satisfy the assumptions of the theory. For given geometry, the assumption of hydraulic control gives a relationship between the

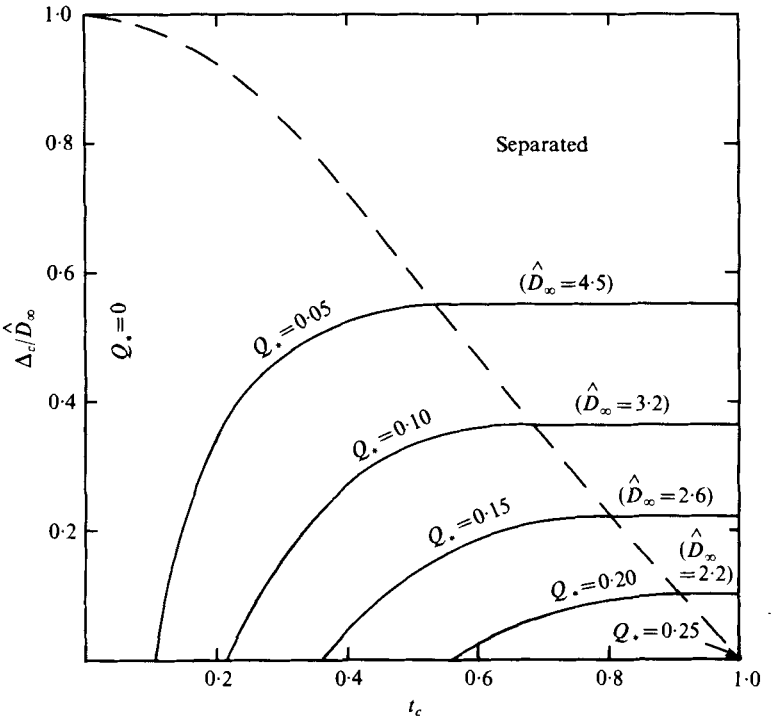

FIGURE 8. Dependence of the non-dimensional flow rate $Q_* = \frac{1}{2}fQ/gD_\infty^2 = \hat{D}_\infty^{-2}$ on geometry for hydraulically controlled flow when $\hat{\psi}_i = \frac{1}{2}$. The abscissa variable is t_c, the hyperbolic tangent of the width of the control section divided by the Rossby radius $(gD_\infty)^{\frac{1}{2}}/\frac{1}{2}f$. The ordinate variable is the ratio of the height Δ_c of the channel floor at the control section to the upstream mid-channel depth D_∞.

conditions at the upstream end of the exit channel. This relationship can then be used as a boundary condition for the basin flow.

The behaviour of the system may depend not only on what processes are important in the basin (e.g. friction) but also on the way in which the flow is established. Consider, for instance, the following situation. Suppose that there is a large basin of constant depth with an exit channel of slowly varying width and depth. This basin is initially filled with inviscid fluid at rest held back by, say, a partition at the sill. What flow develops when this partition is removed?

One might expect the early stages to be something like the behaviour found for a flat-bottomed channel of constant width when there is a small discontinuity in level (Gill 1976). In this case, waves move out from the discontinuity in level, the fastest ones having speed $(gD)^{\frac{1}{2}}$. After the waves have passed by, the outflow is found to be all along the left bank when the channel is wide compared with the Rossby radius. The associated depression in surface level is created by the passage upstream of a Kelvin wave, which can only move along this side of the channel. The next stage in the process would be an adjustment produced by advection of upstream potential vorticity along the left bank by the current. This would presumably lead eventually to a steady flow of the type studied in this paper with $\hat{\psi}_i = \frac{1}{2}$, corresponding to the flow upstream being entirely along the left bank.

A feature of this flow (assuming that the basin is large enough) is that the upstream

interior level D_∞, and hence the upstream potential vorticity, remains at its initial value. The problem, therefore, is to find how the flux Q depends on the height Δ_c of the sill and on the width w_c of the control section. The results (obtained as described in §9) are shown in figure 8 as contours of the non-dimensional flux

$$Q_* = \tfrac{1}{2}fQ/gD_\infty^2 = \hat{D}_\infty^{-2}$$

defined by (4.19). This is shown as a function of t_c, the hyperbolic tangent of the width (in units of the Rossby radius), and of

$$\Delta_c^* = \Delta_c/\hat{D}_\infty,$$

the ratio of the sill height to the upstream interior depth.

The results shown in figure 8 have quite straightforward properties. For instance, the flux tends to zero as the width of the control section tends to zero. The flux increases with increasing width and decreasing sill height, the largest possible value being $\frac{1}{2}gD_\infty^2/f$, for zero sill height and infinite width. When the channel is wide enough, or the sill is high enough, the flow at the control section is separated from the left bank. In these circumstances, changes in width do not affect the flux so Q_* depends only on Δ_c^*. This dependence is given by (10.5).

12. Some sample surface configurations

To give an idea of the variety of solutions possible, a sample set of surface configurations is depicted in figure 9. The first three diagrams are for the same geometry, with a relatively low sill. It is convenient to discuss these diagrams in terms of dimensional variables because the scales introduced in §4 are not fixed for a fixed geometry.

The width w is taken to vary with downstream distance y according to the formula

$$w/w_c = 1 + y^2, \tag{12.1}$$

w_c being the width at the narrowest section. The exact form of this dependence is immaterial as y enters the problem only parametrically. (In other words, it is the profile dependence on w that matters, not the profile dependence on y.) In the low-sill cases the height Δ of the channel floor is given by

$$\Delta = 0{\cdot}25d_w(1+y^2)^{-1}, \tag{12.2}$$

while in the high-sill cases the formula is

$$\Delta = 4{\cdot}0d_w(1+y^2)^{-1}, \tag{12.3}$$

where

$$d_w = (4fw_c)^2/g. \tag{12.4}$$

Case (*a*) is an example where the upstream depth D_∞ is fairly large, giving a large Rossby radius. Hence the narrow-channel approximation is appropriate. The value of t_c is, in fact, 0·4, which is not small enough to make (10.11) very accurate, but it gives the flux to within 20%. The actual value of the flux is $4{\cdot}8q_w$, where

$$q_w = (\tfrac{1}{2}f)^3 w_c^4/g. \tag{12.5}$$

The term involving f on the right-hand side of (10.11) is fairly small, indicating that rotation is having little influence on the flow rate. It does, however, give quite a large tilt to the surface, and separation occurs quite soon after the control section.

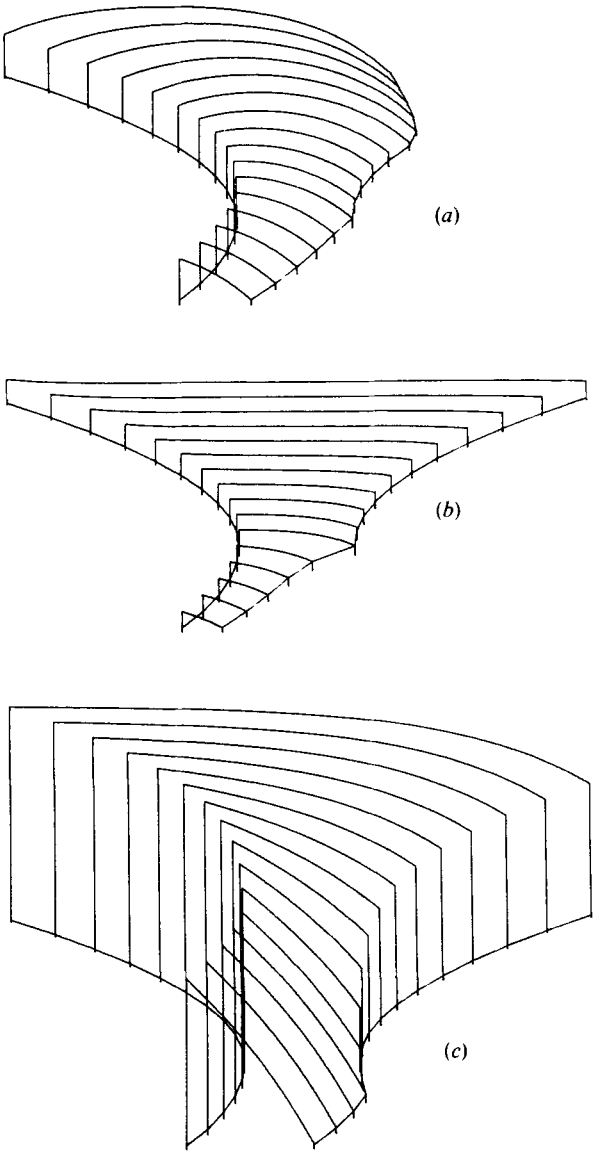

FIGURE 9. Solutions showing the surface configuration for controlled flow in a channel whose width w varies parabolically with downstream distance y (positive out of the page). There are two different geometries. Cases (*a*)–(*c*) correspond to a low sill, the height Δ of the channel floor being given by $\Delta = 0{\cdot}25d_w(1+y^2)^{-1}$, where d_w is given by (12.2). Cases (*d*) and (*e*) correspond to a high sill, with Δ given by $\Delta = 4{\cdot}0d_w(1+y^2)^{-1}$. The flow is determined by the upstream parameters $\hat{\psi}_i$ and $\hat{D}_\infty$, which have the following values: (*a*) $\hat{\psi}_i = 0{\cdot}5$, $\hat{D}_\infty = 2{\cdot}6$ ($D_\infty = 5{\cdot}6d_w$), (*b*) $\hat{\psi}_i = -0{\cdot}5$, $\hat{D}_\infty = 2{\cdot}26$ ($D_\infty = 0{\cdot}5d_w$), (*c*) $\hat{\psi}_i = 3$, $\hat{D}_\infty = 3{\cdot}8$ ($D_\infty = 2{\cdot}1d_w$), (*d*) $\hat{\psi}_i = 0{\cdot}5$, $\hat{D}_\infty = 18$ ($D_\infty = 4{\cdot}5d_w$), (*e*) $\hat{\psi}_i = -1$, $\hat{D}_\infty = 0{\cdot}33$ ($D_\infty = 0{\cdot}46d_w$).

Each figure shows the surface profiles at $y = -2{\cdot}0, -1{\cdot}8, \ldots, 0{\cdot}8, 1{\cdot}0$. The vertical lines at the edges go from the free surface to the reference level, which is the level of the channel floor at $y = -\infty$. The level of the floor at other points is shown by a continuous line intersecting the vertical lines at the appropriate heights. In all cases, the surface intersects the channel floor for $y > y_s$, where $y_s < 0$ (separated flow at the control section) for case (*d*), $y_s = 0$ for cases (*b*) and (*c*), and $y_s > 0$ for cases (*a*) and (*e*). In case (*c*), separated flow occurs upstream of the control section as well.

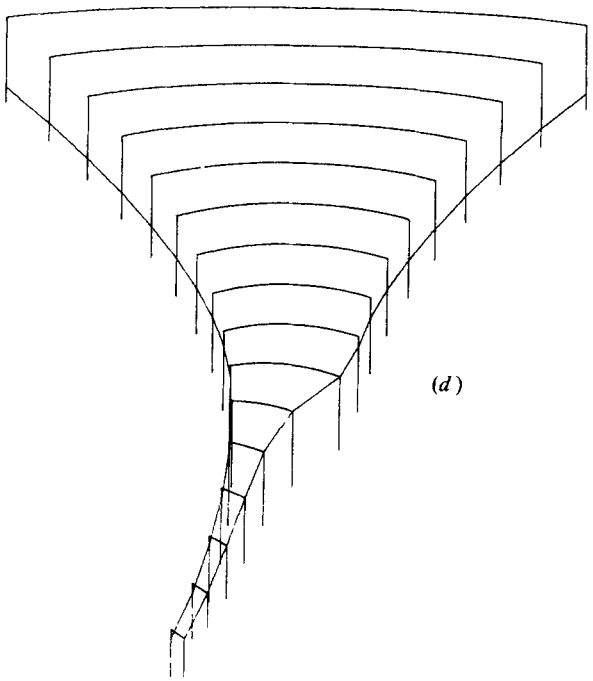

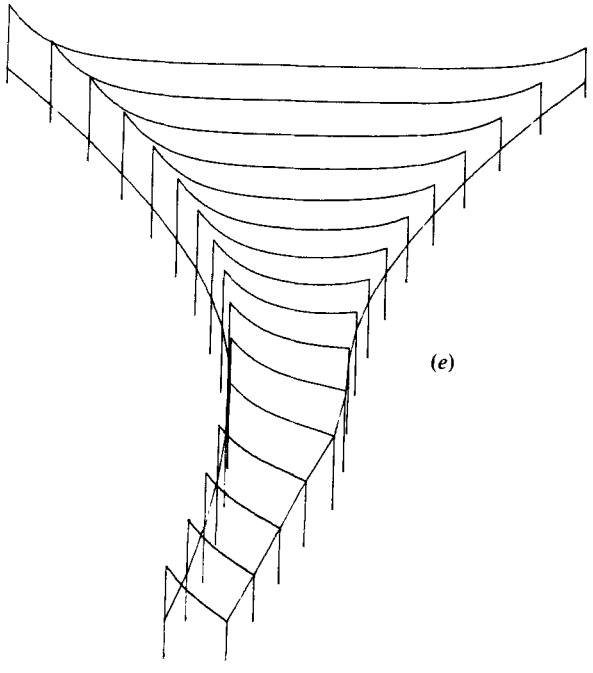

The fact that $y_s > 0$ for case (*e*) is not obvious from the diagram because linear interpolation is used to connect the sections and the separation point lies between $y = 0$ and $y = 0{\cdot}2$. Two different degrees of vertical exaggeration are used in the drawings. Taking the unit of width to be the width of the channel at the narrowest section, the unit of height is $3d_w$ in cases (*a*)–(*c*) and $6d_w$ in cases (*d*) and (*e*).

In cases (*b*) and (*c*), separation occurs at the control section itself, so these examples may be identified with points in figure 7. In case (*b*), the upstream level is low, giving a small Rossby radius, and hence the wide-channel approximation is appropriate ($t_c = 0{\cdot}9$). The flow is very sluggish and the flux is only 1% of the value for case (*a*). Case (*c*) is rather different because of the circulation upstream of the sill. The flux in the left-hand layer towards the sill is equal to $1{\cdot}0q_w$, of which only 30% crosses the sill, the remaining 70% returning in the right-hand layer.

The high-sill examples are shown in figures 9(*d*) and (*e*). In case (*d*), the upstream level is high, being only 20% less than in case (*a*) ($t_c = 0{\cdot}44$). Separation occurs upstream of the control section and so corresponds to a point in the upper part of figure 7. The flux $0{\cdot}069q_w$ is much smaller than in case (*a*) because of the higher sill. It would be more appropriate to say, in fact, that the stream barely manages to cross the sill.

Case (*e*) is another example where there is a circulation upstream of the sill, but in the opposite sense to that in case (*c*). The upstream level is low (as in case (*b*)), making the wide-channel approximation applicable ($t_c = 0{\cdot}9$), and so a point in figure 7 can be identified approximately with this solution. The elevation of the surface at the walls testifies to a large flux. The right-hand layer carries a flux of $2{\cdot}9q_w$ towards the sill, of which $2{\cdot}0q_w$ crosses the sill and the remainder returns in the left-hand layer. The large flux in the approaching stream is necessary to carry fluid across the sill because the general upstream level is well below (about 12%) that of the sill. Note that the surface is concave upwards even at the constriction. Separation does not occur at the constriction itself, but does happen soon afterwards.

13. Discussion

The foregoing analysis leads to a family of steady solutions satisfying certain assumptions. It does not give information about how such a flow might be set up, or indeed whether a flow satisfying these assumptions would ever be set up from given initial conditions. However, one can make reasonable inferences about the two types of problem usually treated in the non-rotating case, namely (*a*), given an initial upstream level, what will be the discharge rate and (*b*), given the rate of supply of fluid to a reservoir, what will be its upstream level? The former problem was discussed in §11. The latter problem appears at first sight to be unresolved since, for any specified outflow, there is a whole family of controlled solutions corresponding to the different values of $\hat{\psi}_i$. This arises, however, because the upstream flow is divided between two boundary layers which are independent of each other. Hence it is permissible to specify the flux in *each* of these boundary layers independently. For instance, one could have a large reservoir of constant depth (to give uniform potential vorticity) and then establish currents in both boundary layers by some sort of forcing. This could be achieved, for instance, by a wind stress parallel to the boundary. The associated Ekman flux raises or lowers the surface level at the boundary and thereby establishes a boundary current (cf. Gill & Clarke 1974).

The above argument seems reasonable if the forcing is such as to produce boundary currents. However, if a source is specified in the *interior* of a basin (e.g. as a model of bottom water formation giving rise to a source of deep water as in the Greenland Sea), the problem has a different character. When fluid is introduced into a rotating system, it behaves quite differently from the non-rotating case because fluid particles tend to

move no more than a Rossby radius from their initial position. Thus the fluid remains confined to a dome-shaped region with motion following contours of fluid depth. If the fluid is inviscid, outflow from the basin will not occur until the dome has become so large that its effective Rossby radius is comparable with the basin width and the skirts of the dome reach the exit channel. In practice, however, friction will modify the flow and tend to spread out the dome. In this case, it may be possible to find a solution where friction is important in the basin, but not in the immediate neighbourhood of the sill, where hydraulic control takes place.

The results of this paper are identical with those of Whitehead *et al.* (1974) in the limit of zero potential vorticity, and their use of a maximization principle to determine the hydraulically controlled flow is supported by the conclusions reached above. The maximization principle corresponds, in fact, to an application of (3.3). They write their flow equation in the form

$$Q = G(h, w, \ldots; D), \tag{13.1}$$

where Q is the flow rate and their choice of flow variable D is the variable they call h_0. So, taking $\mathscr{J} = Q - G$, (3.3) gives $\partial G/\partial D = 0$, which is the principle they used. Stern's (1974, 1976) method is yet another form, where Q in (13.1) is replaced by the width of the constriction. The experiments of Whitehead *et al.* (1974) were in good agreement with the theory despite the experimental arrangement, which involved sudden changes in width and depth at the entrance to their channel. Experiments have also been reported by Sambuco & Whitehead (1976), but their geometry did not satisfy the assumptions of the theory.

These results show the feasibility and usefulness of laboratory experiments in studying hydraulically controlled flows, and this paper indicates that there is a wide range of flow regimes yet to be explored.

There seem to be a number of sills in the ocean where hydraulic control concepts are applicable. The main point of the theory is that it selects that solution for which the flow upstream of the control is fundamentally different from that downstream of the control (i.e. control is at a change of branch). The observed situation shown in figure 1 obviously has this character, and estimates of the Froude number by Stalcup, Metcalf & Johnson (1975) support the idea of hydraulic control. Similar arguments apply to flow through the Denmark Straits, which was discussed by Whitehead *et al.* (1974). Therefore the outstanding issues concern not whether hydraulic control is taking place, but how the solution is affected by the stratification and local topography, and how it is related to the upstream flow. For instance, what determines the upstream potential vorticity and what determines the way the flow is subdivided between the two upstream boundary layers? How much do mixing and friction affect the solution? When do features like hydraulic jumps occur? There are also interesting questions about the nature of the flow downstream of the control. This problem has been studied by Smith (1975) in connexion with the overflow from the Norwegian Sea and from the Mediterranean.

The analysis carried out in this paper was limited to determining the effect of geometry and upstream conditions on the nature of the flow. The range of solutions obtained was somewhat restricted by the assumptions of uniform potential vorticity and of rectangular cross-sections, but was sufficiently wide to give an interesting variety of behaviour, as is evident from figure 9.

The methods used are capable of a great deal of generalization, as some exploratory investigations have shown. For instance, the choice of a rectangular cross-section was merely one of convenience, and it is not difficult to treat other shapes of channel floor. It is not even necessary to have a channel with two sides, as hydraulic control can be induced in a boundary current by topographic effects which may be localized to the boundary region. This gives an indication of how coastal currents in the ocean, for instance, can be affected by changes in the cross-sectional shape of the continental shelves. For such applications, the one-layer model is rather unrealistic, but it is straightforward to generalize the methods to two or more layers. The assumption of constant potential vorticity can also restrict appicability to real situations. However this can be overcome by models with piecewise constant potential vorticity. The feature of the analysis which would not be easy to change is the slowly varying assumption, because this allows flow profiles at different sections to be calculated independently. This eliminated dependence on position in the cross-section from the problem, so leading to equations involving only downstream distance and time.

I should like to thank Mr Julian Smith for computing solutions and producing the computer drawings displayed in figure 9.

Appendix

In §9 it was stated that flow in the control section is always unidirectional. The proof of this statement for the non-separated case will now be given. By §7, a necessary and sufficient condition for unidirectional flow is that $|r| \leqslant 1$. The proof that this condition is satisfied at the control section follows in two stages.

(*a*) *Proof that* $r \geqslant -1$. Using (9.6) to substitute for $\hat{D}_\infty$ in the expression (7.6) for r, one obtains at the control section

$$r = \frac{t_c^2 \bar{D}^4 - 4}{(1-t_c^2)\,\bar{D}_c^2} \geqslant \frac{t_c^2 - 1}{(1-t_c^2)\,\bar{D}_c^2} = -\frac{1}{\bar{D}_c^2} \geqslant -1$$

since $\bar{D}_c \geqslant 1$ for a non-separated flow.

(*b*) *Proof that* $r \leqslant 1$

$$r = t_c^2 \bar{D}_c^2 - \frac{(1-t_c^4\,\bar{D}_c^4)}{(1-t_c^2)\,\bar{D}_c^2} \leqslant 1$$

since (9.6) requires $\bar{D}_c t_c \leqslant 1$ in order for $\hat{D}_\infty$ to be positive.

REFERENCES

BINNIE, A. M. 1949 *Proc. Roy. Soc.* A **197**, 545.
GILL, A. E. 1976 *J. Fluid Mech.* **77**, 603.
GILL, A. E. & CLARKE, A. J. 1974 *Deep-Sea Res.* **21**, 325.
HUGONIOT, P. H. 1886 *C. R. Acad. Sci., Paris* **103**, 1178.
LONG, R. R. 1972 *Ann. Rev. Fluid Mech.* **4**, 69.
REYNOLDS, O. 1886 *Phil. Mag.* (5) **21**, 185.
SAMBUCO, E. & WHITEHEAD, J. A. 1976 *J. Fluid Mech.* **73**, 521.
SMITH, P. C. 1975 *Deep-Sea Res.* **22**, 853.
STALCUP, M. C., METCALF, W. G. & JOHNSON, R. G. 1975 *J. Mar. Res. Suppl.* **33**, 15.
STERN, M. E. 1974 *Geophys. Fluid Dyn.* **6**, 127.
STERN, M. E. 1976 *Ocean Circulation Physics.* Academic Press.
WHITEHEAD, J. A., LEETMAA, A. & KNOX, R. A. 1974 *Geophys. Fluid Dyn.* **6**, 101.